Environmental Modelling and Software 116 (2019) 100–109

Contents lists available at ScienceDirect

Environmental Modelling & Software

journal homepage: www.elsevier.com/locate/envsoft

A statistical physics approach to perform fast highly-resolved air quality simulations – A new step towards the meta-modelling of chemistry transport models

Bertrand Bessagnet[a,b,*], Florian Couvidat[a], Vincent Lemaire[a,c]

[a] National Institute for Industrial Environment and Risks, Parc Technologique ALATA, 60550, Verneuil-en-Halatte, France
[b] Hangzhou Futuris Environmental Technology Co. Ltd, Zhejiang Overseas High-Level Talent Innovation Park, No. 998 WenYi Road, 311121, Hangzhou, Zhejiang, China
[c] Center for Climate and Resilience Research (CR)2, Departamento de Geofísica, U. de Chile Blanco Encalada, 2002, Santiago, Chile

ARTICLE INFO

Keywords:
Air quality modelling
Linear regression
Statistics
Metamodel
Resolution
Increment

ABSTRACT

A methodology rested on model-based machine learning using simple linear regressions and the parameterizations of the main physics and chemistry processes has been developed to perform highly-resolved air quality simulations. The training of the methodology is (i) completed over a 6-month period using the outputs of the chemical transport model CHIMERE, and (ii) then applied over the subsequent 6 months. Despite rough assumptions, this new methodology performs as well as the raw CHIMERE simulation for daily mean concentrations of the main criteria air pollutants (NO_2, Ozone, PM10 and PM2.5) with correlations ranging from 0.75 to 0.83 for the particulate matter and up to 0.86 for the maximum ozone concentrations. Some improvements are investigated to expand this methodology to several other uses, but at this stage the method can be used for air quality forecasting, analysis of pollution episodes and mapping. This study also confirms that including a minimum set of selected physical parameterizations brings a high added value on machine learning processes.

1. Introduction

Air pollution is the fourth leading fatal risk for human health globally, and in the latest estimates, more than 5 million pre-mature deaths are linked with air pollution (Forouzanfar et al., 2016). Air pollution does not just cause danger to human health but also to the environment, the economy and food security (*e.g.* crop yield losses). Chemistry transport models (CTMs) are useful tools to assess, predict and analyse environmental policies to improve air quality. Since a large fraction of the population live in urban areas, models must run up to the urban scale. The model outputs can feed integrated models to assess emission reduction strategies up to the local scale (Amann et al., 2017; Anil et al., 2018).

In atmospheric sciences the race on high resolution simulations over large domains started few years ago for short term forecast or climate studies perspectives (Skamarock et al., 2014; Fuhrer et al., 2018). In a near future, meteorological 3D-fields will be commonly available over large domains at a few kilometers resolution. For air quality modelling, increasing the resolution is expected to provide better results. Even for remote background sites, increasing the resolution should improve the quality of simulations because the system is not fully linear mainly due to the use of non-linear chemistry schemes. The use of air quality models at high resolution is very computing time consuming mainly because of Courant–Friedrichs–Lewy (CFL) conditions. The CFL condition is a necessary condition for convergence while solving certain partial differential equations numerically by the method of finite differences. This condition imposes to adapt the time step. For the advection, it is proportional to the grid size for the horizontal transport involving a dramatic increase of simulation durations. Although a 20 km–50 km resolution is sufficient to be representative of rural background concentrations, the use of resolution between 1 and 10 km is essential to estimate urban background concentrations of pollutants for small to large cities.

The notion of urban increment (or decrement for ozone due to the titration effect) has been introduced to estimate the impact of a city emissions to the urban background concentrations (Amann et al., 2007; Ortiz and Rainer, 2013). The calculation of this increment is expected to be influenced by local primary emission sources and meteorological parameters. The use of highly resolved bottom-up emission inventory usually provides better results (Timmermans et al., 2013) compared to top-town downscaled emission datasets. Air quality models benefit from a downscaling of emissions dataset as mentioned by Schaap et al.

* Corresponding author. National Institute for Industrial Environment and Risks, Parc Technologique ALATA, 60550, Verneuil-en-Halatte, France.
E-mail address: bertrand.bessagnet@futuris-environment.com (B. Bessagnet).

https://doi.org/10.1016/j.envsoft.2019.02.017
Received 9 September 2018; Received in revised form 18 December 2018; Accepted 19 February 2019
Available online 27 February 2019
1364-8152/ © 2019 Elsevier Ltd. All rights reserved.

(2015), Terrenoire et al. (2015) and Colette et al. (2014) by mainly reducing the bias over urbanized areas with sometimes lower correlations. However, for ozone an optimal resolution could be found as explained by Valari and Menut (2008) based on an analysis of the root mean square error. In a scenario perspective the concept of urban and even street increment was used in Kiesewetter et al. (2014, 2015) to estimate the impact of emission reductions strategies at a given site, up to traffic-influenced stations.

In previous studies, the use of past observational air quality data crossed with predicted meteorological variables, traffic emission prediction was implemented in neural networks to propose statistical models able to perform air quality model predictions (Catalano and Galtioto, 2017 and references therein). Usually, these models can only be used at a given site, but they offer robust performances. Recently, Mallet et al. (2018) proposed a first metamodel of a local air quality model to simulate NO_2 and PM10 concentrations.

In our study, the concept of "urban increment" is extended to "grid cell increment" to perform highly-resolved air quality simulations rested on model-based "machine learning" using low resolution CTM simulations. This method avoids running the CTM at high resolution and therefore allows an impressive gain of computing time. This technique is applied for the main criteria pollutants PM10, PM25, NO_2, and O_3 concentrations. The method is evaluated for daily or maximum concentrations (for ozone only). This paper will answer four main questions: Does this technique provide satisfactory results by-passing the costly high resolution air quality simulation? What is the expected gain on computing time? For which type of application this technique can be used? How this technique could be improved?

2. Material and methods

2.1. Model set-up

In this study, the CHIMERE model (Menut et al., 2013, Mailler et al., 2017) as improved in Couvidat et al. (2018) is used over two domains: (i) a domain (**EU**) encompassing Europe at 0.5° × 0.25° regular resolution (**LRE**) over the 17°E − 40°W and 32°N – 70N window, and (ii) a nested domain (**FR**) centered over France at 0.09375° × 0.046875° regular resolution (**HRE**) over 5°E − 10°W and 41°N – 51.014 625°N fed by the EU simulation (one-way nesting). The model configuration is summarized hereafter, but the reader can refer to the recent CHIMERE publications (Couvidat et al., 2018; Bessagnet et al., 2017, Mailler et al., 2017) for details on the corresponding model components and references as well as non-user-specific model characteristics. The particle size ranges from 10 nm to 10 μm over 9 bins according to these ranges from bin n°1 to bin n°9 which are respectively [10.00 nm - 22.01 nm], [2.20 nm - 48.43 nm], [48.43 nm - 106.7 nm], [106.7 nm - 234.7 nm], [234.7 nm - 516.2 nm], [516.2 nm - 1.14 μm], [1.14 μm - 2.50 μm], [2.5 mm - 5.0 μm], [5.0 μm - 10.0 μm]. In this study, the major PM species are considered: secondary inorganic aerosol (nitrate, sulfate and ammonium), secondary organic aerosols (anthropogenic and biogenic in origins), natural mineral dust, sea salt and Primary Particle Matter.

Horizontal transport is solved with the second-order Van Leer scheme (Van Leer, 1979). Subgrid scale convective fluxes are considered. Once the depth of the boundary layer is computed, vertical turbulent mixing can be applied following the k-diffusion framework after the parameterisation (without counter-gradient term) of Troen and Mahrt (1986) detailed in Menut et al. (2013). A minimal vertical eddy diffusion k is assumed with values of 0.01 $m^2 s^{-1}$ in the dry boundary layer and 1 $m^2 s^{-1}$ in the cloudy boundary layer. k is capped to a maximal value of 500 $m^2 s^{-1}$ to avoid unrealistic mixing. Above the boundary layer, a fixed value of 0.1 $m^2 s^{-1}$ is used. The present setup also benefits from an improved representation of turbulent mixing in urban areas that yields lower horizontal wind and vertical mixing in order to better capture the difference between the urban canopy (where the first CHIMERE model level lies) and the top of the urban sublayer of which the lowermost meteorological model level is representative (Terrenoire et al., 2015). As an offline chemistry transport model, CHIMERE requires prescribed meteorological fields which were provided here by ECMWF with the Integrated Forecasting System (IFS) model at 0.125° resolution with data assimilation. Although the study is performed in a forecasting perspective, meteorological data are issued from reanalyzes. Emissions of the main pollutants are issued from EMEP (Cooperative programme for monitoring and evaluation of long range transmission of air pollutants in Europe) programme available at http://www.emep.int. Over France the spatialization of emissions is performed with a 1 km proxy based on the national bottom-up emission inventory (accessible at http://emissions-air.developpement-durable.gouv.fr/) that feeds the emission pre-processor of CHIMERE described in Mailler et al. (2017).

2.2. Air quality simulations

A complete CHIMERE simulation for the EU and FR domains is performed from 1st July 2010 to 30 June 2011 (1 year) with a 10-day spin-up period in June 2010 for the initialization. As explained in Mailler et al. (2017), the CHIMERE simulation is divided in two main steps:

- **Step (1)**: A pre-processing to prepare intermediary files from raw data for meteorology, emissions, boundary conditions. This step consists in performing horizontal, vertical and time interpolations and calculation of diagnostic variables (*e.g.* the vertical mixing coefficient). So far, this step is computed in a sequential way using only one processor.
- **Step (2)**: The core CHIMERE simulation, which uses the previous intermediary files, provides the main model outputs on an hourly frequency. This computing step is parallelized, but this step is the costliest and it can roughly represent 80–90% of the total computing time depending on the number of processors and the size and grid resolution of the domain.

The increment methodology described hereafter is a two steps method with (i) a training part for a given version of the CHIMERE model on a given period (here 6 months in 2010) and (ii) an application part on another period of interest (here 6 months in 2011). All the programs are written in shell language using the NCO package (Zender, 2008) to efficiently handle output NETCDF files. The method is depicted in Fig. 1 and fully explained in the next subsections. In this study, the two distinct periods are defined:

- The "training period" from 1st July 2010 to 31 December 2010 where the "increment methodology" called **FR_INC** (applied over the FR domain) is trained to cover a large range of meteorological conditions: summer, winter and intermediate seasons. This "learning" process uses the CHIMERE simulation outputs and intermediary variables over the EU and FR domains (EU_LRE and FR_HRE simulations).
- An "evaluation period" from 1st January 2011 to 30 June 2011, where the "increment technique" is evaluated against observations and compared with the high resolution CHIMERE simulation (**FR_HRE**). This period covers the full spring period with usual high PM concentrations in the western part of Europe.

2.3. Principle of the increment methodology

Based on atmospheric diffusion theory, potential determinants of urban increments and functional forms of their relationships have been hypothesized. Under neutral atmospheric conditions, the vertical diffusion of a non-reactive pollutant from a continuous point source can be described in general form through the following relationship (Amann et al., 2007; Seinfeld and Pandis, 1998):

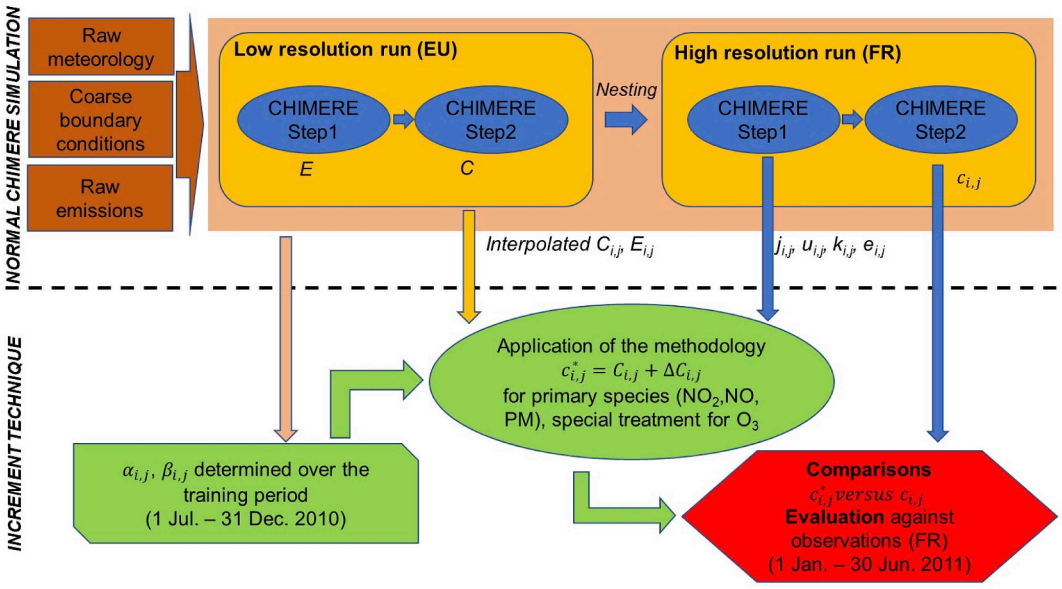

Fig. 1. Synoptic scheme of the increment technique compared to the normal CHIMERE simulation over the EU and FR domains. All variables are explained in sections 2.3 and 2.4.

$$\sigma_z^2 = \frac{2kx}{u} \tag{1}$$

with σ_z^2 (m^2) indicating the variance of the vertical diffusion after a distance x from the source, k ($m^2\ s^{-1}$) as the eddy diffusivity and u (m s^{-1}) the wind speed. Considering this assumption, in Amann et al. (2011) the delta between urban and background concentrations ΔC of primary PM is given as:

$$\Delta C = \frac{\sqrt{d}}{\sqrt{8ku}} Q \tag{2}$$

d is the characteristic length of the city, Q (μg $m^2\ s^{-1}$) is the low level emissions of the city. This increment must be corrected to avoid emission double counting as explained in Amann et al. (2011). Based on Amann et al. (2011) and Amann et al. (2007), we consider in this study that a given fine cell can behave as a "city". Then, the concentration delta (ΔC) between a fine grid and a coarse grid simulation of a species concentration influenced by low level sources of primary pollutants can be extended with a revised predictor variable as:

$$\Delta C = c - C = \alpha \frac{1}{\sqrt{ku}} (e\sqrt{d} - E\sqrt{D}) + \beta$$
$$\mathrm{d} \propto \sqrt{\delta x \delta y}$$
$$\mathrm{D} \propto \sqrt{\delta X \delta Y} \tag{3}$$

- c and C (μg m^{-3}) are respectively the concentrations at the fine grid point and interpolated from the coarse grid to the fine mesh, k is the vertical mixing coefficient ($m^2\ s^{-1}$) at the fine grid, u is the 10 m horizontal wind speed (m s^{-1}) at the fine grid, δX, δY, δx, δy are respectively the coarse longitude, latitude and the fine longitude, latitude increments of the grids (°). In our study they are constant, but they can vary and for each fine grid cell an average value of the surrounding coarse grids can be used.

- d and D are characteristic lengths respectively for the fine and coarse meshes, they correspond here to an average of the grid cells size

- e and E (μg $m^{-2}\ s^{-1}$) are respectively the low-level emission fluxes at the fine grid point and interpolated from the coarse grid. For the PM2.5 and PM10 concentrations, the sum of primary emissions is considered, for NO and NO_2 the NOx emissions are considered. In our methodology, the emissions of the two first level (sum of emissions approximatively below 30 m) of CHIMERE are taken into account.

- α and β are coefficients integrating geographical, physical and chemical processes that are lost in the simplification process, they also account for unit changes. Note that *β here has not the same meaning than in* Amann et al. (2007, 2011), it is here residual value of the regression and would be expected to be close to 0.

Differently to Amann et al. (2007) the vertical eddy diffusion k is not integrated in the α coefficient but included in the predictor $\frac{1}{\sqrt{ku}}(e\sqrt{d} - E\sqrt{D})$, because this variable is calculated and stored during the CHIMERE preprocessing. Moreover, in our methodology, E includes all low level emission sources in the coarse grid and can be eventually higher than e if the grid cell is in a remote areas surrounded by high emissions area. This change is to break the implicit assumption assumed in Amann et al. (2007, 2011) that background concentrations could be only influenced by the city emissions (here the high resolution grid cell). It is then noteworthy that in the case of a fine grid cell with low emissions compared to higher background concentrations the predictor could turn negative which makes intuitively sense while in Amann et al. (2007, 2011) the delta is always positive at it refers to a city implicitly influenced by lower background concentrations.

The principle of our methodology is to calculate on a daily basis these two coefficients α and β for each fine grid cell on the "training" period where all the other variables are known. The previous formula (Eq. (3)) is used for primary PM, NO and NO_2 concentrations, the main assumption is to neglect chemistry processes that are partially included in α and β and also included in the low resolution CHIMERE outputs.

2.4. Application of the methodology

2.4.1. Treatment of PM2.5, PM10, NO_2 and NO

This "increment methodology" is then applied for PM2.5, PM10, NO_2 and NO hourly ground concentrations over the "evaluation period" from 1st January to the 30 June 2011 with the α and β coefficients computed over the "training period" (Fig. 1):

$$c^*_{i,j} = C_{i,j} + \Delta C_{i,j}$$
$$\Delta C_{i,j} = \alpha_{i,j} \times \widetilde{\Delta C_{i,j}} + \beta_{i,j}$$
$$\widetilde{\Delta C_{i,j}} = \frac{1}{\sqrt{k_{i,j} u_{i,j}}} (e_{i,j}\sqrt{d} - E_{i,j}\sqrt{D}) \tag{4}$$

with c^* the concentration on the fine mesh determined by the

Table 1
Limits of concentrations to avoid overshoots when applying the increment technique on hourly values.

	ΔC Limit inf	*ΔC Limit sup*	*c* limit inf*	*Unit*
NO_2	−5	+50	0.1	ppb
NO	−5	+75	0.01	ppb
PM10	−5	+50	1.0	μg m^{-3}
PM2.5	−5	+40	0.75	μg m^{-3}
O_3	–	–	0.1	ppb

increment technique, C the interpolated coarse grid concentration on the fine mesh, i and j referring to the coordinates indexes of a given fine mesh grid cell. $\widetilde{\Delta C}$ is the predictor variable and ΔC the increment value applied to the background concentration value C as discussed in the previous section. The other variables were previously defined, e, E, k and u are computed during the first step of the CHIMERE preprocessing as depicted in Fig. 1.

2.4.2. Special treatment for Ozone

For a secondary pollutant like ozone involved in a non linear chemistry scheme, the previous formulas (Eq. (3) and (4)) based on delta of concentrations are not suited. During et al. (2011) proposed a simplified stationary model to estimate ozone and NO_2 concentrations influenced by low level sources like traffic emissions. The main two equations of the ozone chemistry involving NOx and Ozone are:

$$NO + O_3 \xrightarrow{k_r} NO_2 + O_2$$

$$NO_2 \xrightarrow{J} NO + O_3$$

with J (s^{-1}) the photolytic frequency of NO_2, k_r ($ppb^{-1}\,s^{-1}$) the kinetic rate. The differential equations describing the reactions of NO_2, NO, and O_3 with a diffusion term due to transport and mixing gives:

$$\frac{d[O_3]}{dt} = -k_r[NO]\Delta[O_3] + J\Delta[NO_2] + \frac{[O_3]_B - [O_3]}{\tau} \quad (5)$$

The first two terms on the right side describe the chemical transformation by thermal and photochemical reactions. The last term describes the mixing as a function of concentration differences between a background concentration (index B) and the point at which the concentration should be calculated (here on the fine mesh). In a stationary regime assumption with $d[O_3]/dt = 0$ the equation gives for ozone concentration the approximation $\tilde{c}$:

$$\tilde{c}_{[O_3]} = \frac{j\tau c_{[NO_2]} + C_{[O_3]B}}{1 + \tau k_r c_{[NO]}}$$

$$\tau = \sqrt{\frac{\sqrt{\delta x \delta y}}{8ku}}$$

$$j = 1.47 \times 10^{-5} swrd - 4.84 \times 10^{-9} swrd^2$$

$$k_r = 3.9 \times 10^{-4}\ ppb^{-1} s^{-1} \quad (6)$$

$C_{[O_3]B}$ is the interpolated concentration over the fine grid of the low resolution concentrations (EU_LRE), $c_{[NO_2]}$ and $c_{[NO]}$ are the concentrations over the fine mesh (FR). τ is defined in Amann et al. (2007) as a simplification of diffusion for a box model as previously discussed, $\sqrt{\delta x \delta y}$ is an average characteristic length of the grid cell. We considered here j as a polynomial function of the short wave radiation *swrd* (W m^{-2}) as reported in Trebs et al. (2009) for low altitude sites considering an albedo equal to zero. Here we assumed the kinetic rate k_r to be constant. A statistical method similarly to primary pollutants is implemented, two coefficients α and β are computed over the training period:

$$c_{[o3]} = \alpha \times \tilde{c}_{[O_3]} + \beta \quad (7)$$

Over the training period $c_{[o3]}$ is known and $\tilde{c}_{[O_3]}$ can be calculated each hour then α and β are calculated using a simple linear regression for each grid points on a daily basis. This technique suppresses systematic biases and accounts for missing processes due to the

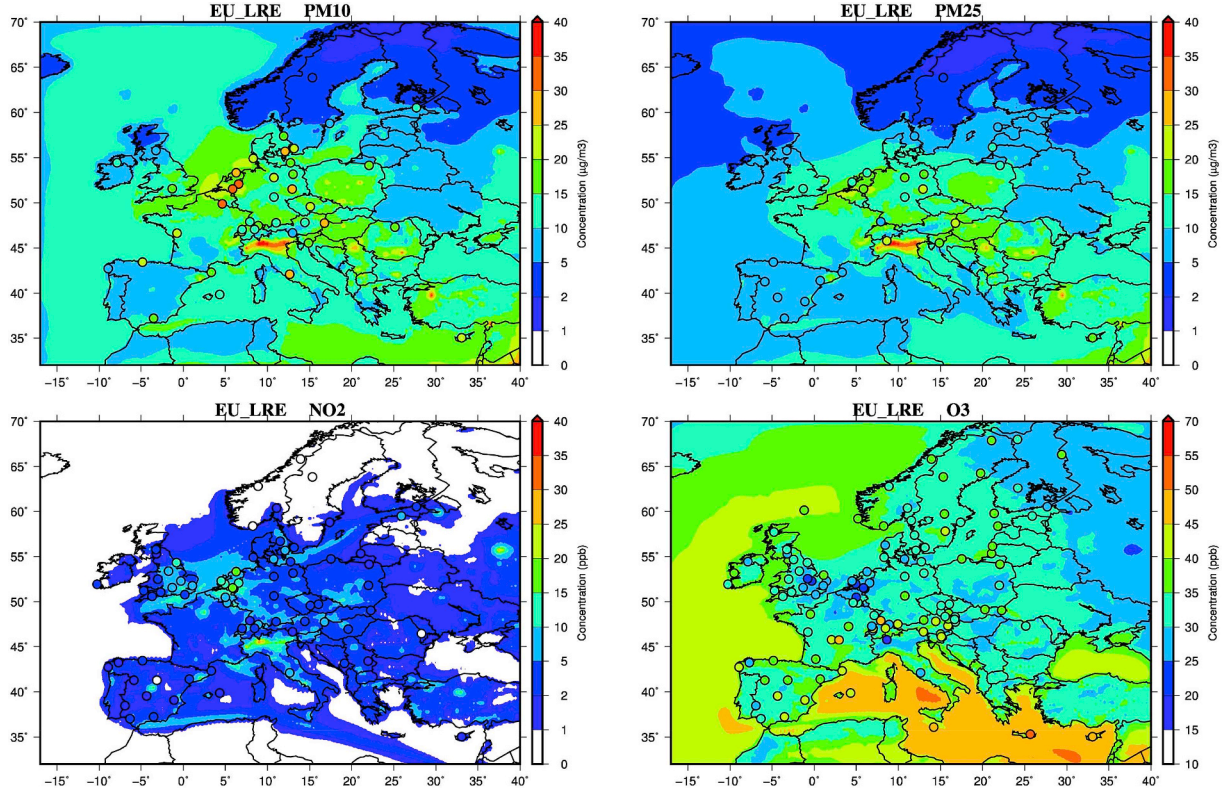

Fig. 2. Maps of mean PM10, PM2.5, NO_2 and O_3 concentrations over the 1st January – 30 June 2011 period for the CHIMERE low resolution simulation at the European scale (EU_LRE). Filled circles represent the rural background observation sites issued from the EBAS database.

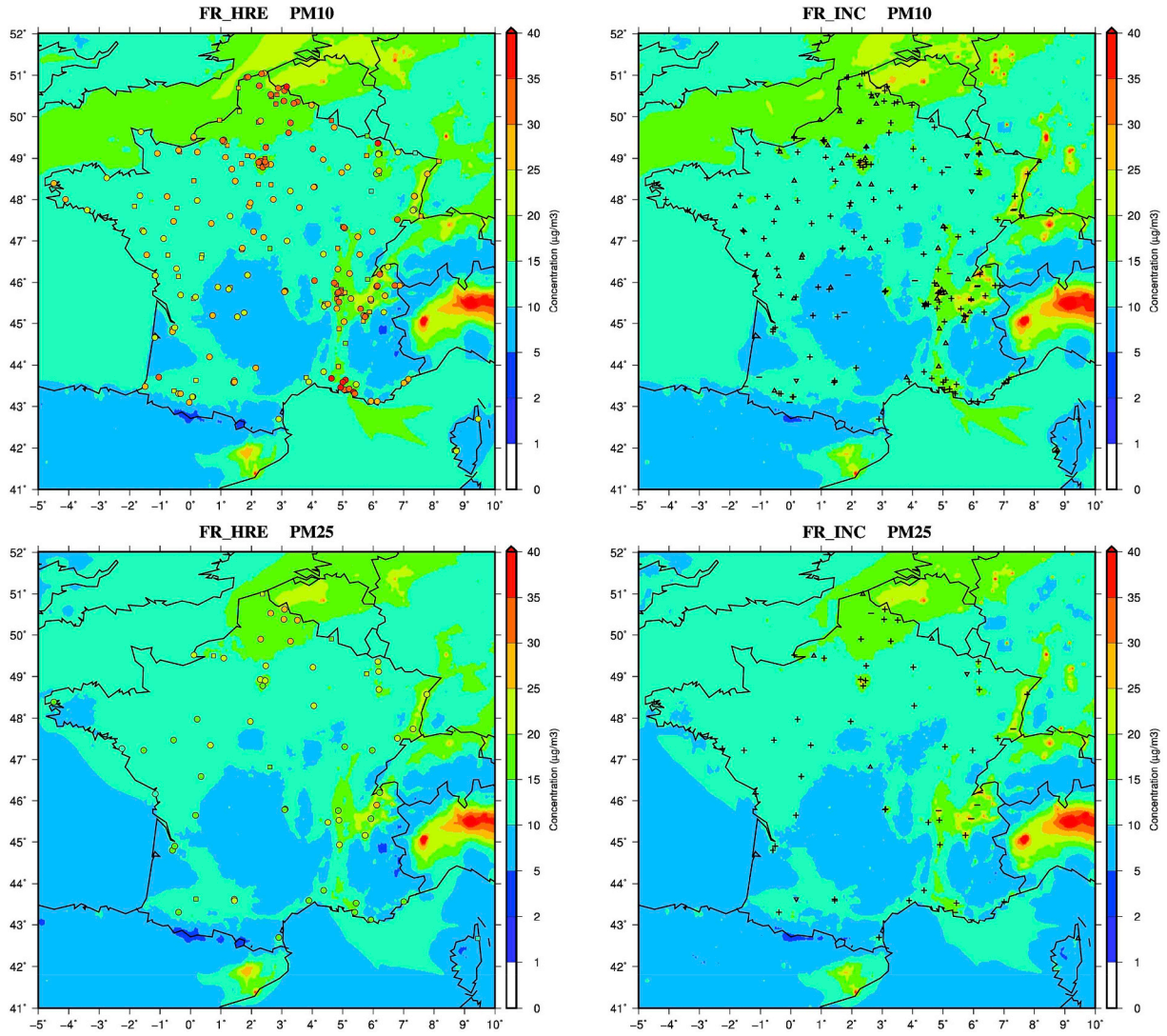

Fig. 3. Maps of mean PM10 and PM2.5 concentrations over the 1st January – 30 June 2011 period for the increment methodology FR_INC (right column) and the CHIMERE high resolution simulation FR_HRE (left column). On the left side: circles and squares filled symbol refer to observations respectively for urban and rural sites. On the right side: bold "triangle up" and "plus" symbols are plotted respectively for rural and urban sites when the increment methodology provides a better Root Mean Square Error compared to the CHIMERE high resolution, bold "triangle down" and "minus" symbols are plotted respectively for rural and urban sites when the increment methodology provides a worse Root Mean Square Error compared to the CHIMERE high resolution.

simplifications. Afterwards, over the evaluation period α and β are applied over hourly concentrations for each grid cell (i,j), then the final ozone concentration c* is simply computed as:

$$c^*_{[O_3]i,j} = \alpha_{i,j} \times \tilde{c}_{[O_3]i,j} + \beta_{i,j} \quad (8)$$

2.4.3. Regression coefficients

To avoid any overshoots when applying the methodology on hourly values, concentrations and delta of concentrations are capped according values reported in Table 1.

In the Supplementary Material Fig. S1, the α (slope), β (intercept) coefficients and the Pearson correlation of the linear regression calculated over the "training" period are reported for all pollutants. For each grid cell the coefficients are calculated using 184 daily values (6 months). The median correlations over the FR domain are 0.31, 0.33, 0.35 and 0.98 respectively for PM2.5, PM10, NO_2 and O_3 with generally higher values over urban areas. The low correlations result from the averaging process over the whole domain where low absolute values in remote areas deteriorate the statistic errors. The correlation is the highest for ozone since the linear regression is based on the absolute concentrations mainly driven by the background values and not a delta of concentrations as for primary pollutants. The α coefficient is generally below 1 confirming the tendency that the high resolution simulation produces lower concentrations compared to the low resolution run.

3. Results and discussion

3.1. Evaluation of the increment methodology

For the European domain (EU), background PM2.5, PM10, NO_2 and O_3 observational data are retrieved thanks to the EMEP-EBAS database (Tørseth et al., 2012). The increment methodology can be evaluated against the raw CHIMERE simulation and observations over the FR domain for the 1st January – 30 June 2011. The French GEOD'AIR database provides hourly concentrations for all stations over France (available online at https://www.geodair.fr/). All background observations are used on a daily basis for the main pollutants: Ozone, NO_2, $PM_{2.5}$ and PM_{10}. Urban, periurban and rural stations are considered, daily maximum concentrations are only considered for Ozone. In this

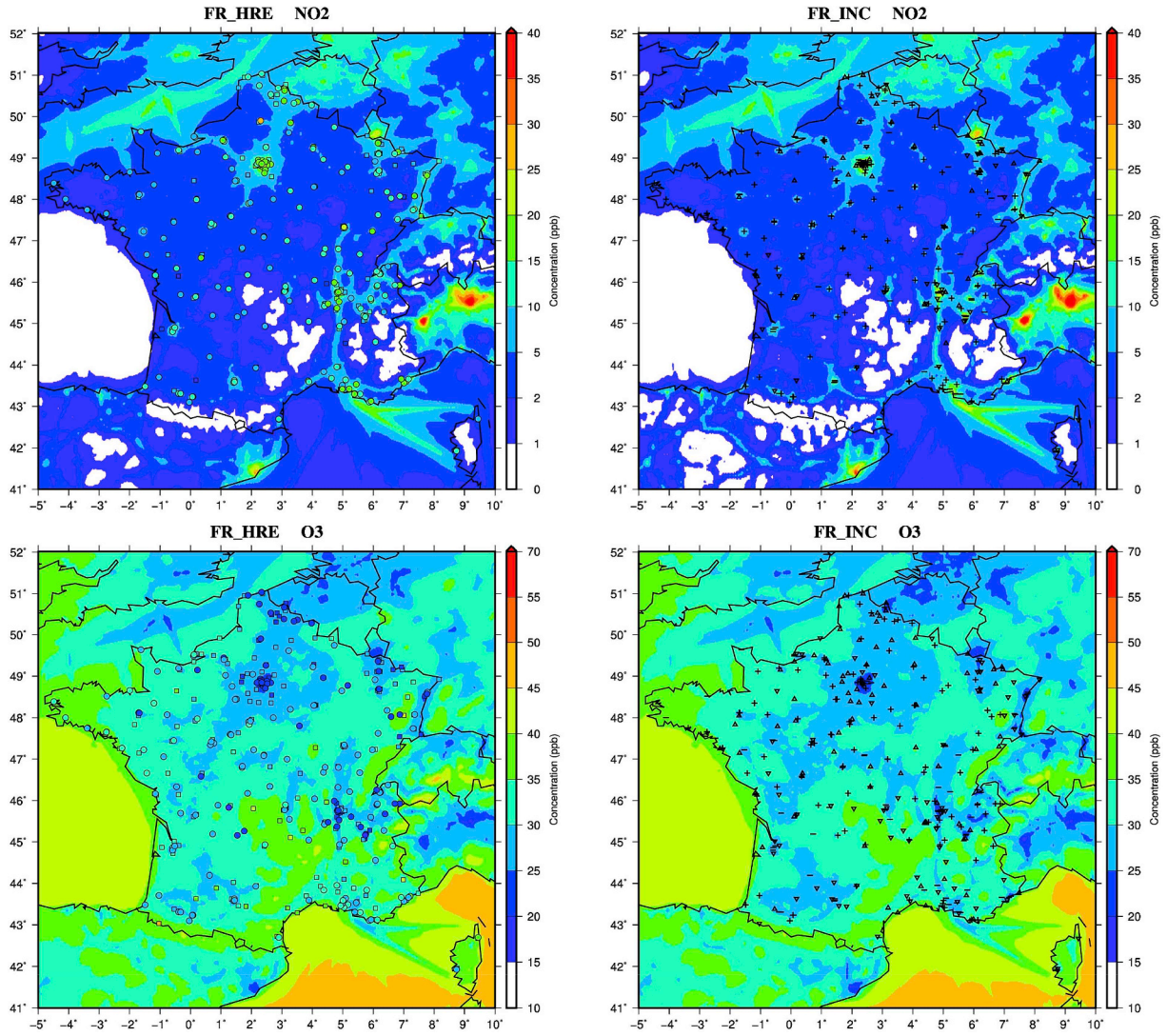

Fig. 4. Maps of mean NO_2 and O_3 concentrations over the 1st January – 30 June 2011 period for the increment methodology FR_INC (right column) and the CHIMERE high resolution simulation FR_HRE (left column). On the left side: circles and squares filled symbol refer to observations respectively for urban and rural sites. On the right side: bold "triangle up" and "plus" symbols are plotted when the increment methodology provides a better Root Mean Square Error compared to the CHIMERE high resolution, bold "triangle down" and "minus" symbols are plotted when the increment methodology provides a worse Root Mean Square Error compared to the CHIMERE high resolution.

paper, periurban and rural are lumped into the category "rural" to better isolate the "urban" signal. Only the French data are considered for the evaluation over the FR domain as we benefit from the most accurate emission data only in France since a bottom-up emission proxy is used over this country.

At the European scale (Fig. 2), CHIMERE is able to retrieve the main patterns of air pollution with the highest concentrations of PM over the Benelux, south of Poland and the north of Italy. The agreement with observations is rather good for PM2.5 concentrations over Spain and UK with a clear underestimation over Benelux. The underestimation of PM is commonly observed in air quality modelling due to the underestimation of emissions (wood burning issue in winter) and weaknesses of models to represent high concentrations of ammonium nitrate during the early spring period (Bessagnet et al., 2016). For O_3 and NO_2 concentrations the model reproduces quite well the observations. Ozone concentrations are usually lower nearby emission areas and the highest over the sea due to accumulation effects and weak deposition over water bodies (confirmed by observations in Malta, Cyprus and Crete), and altitude sites (Massif Central in France and Alps) due to transport of ozone from the free troposphere.

Figs. 3 and 4 show the added value on air quality simulations when using a higher horizontal resolution. Clearly, the regional patterns computed at low resolution are important drivers of the fine resolution outputs for PM and Ozone, however an urban signal is clearly identified for the major cities and in some Alpine valleys mainly due to the effect of stagnant conditions.

Table 2 reports global error statistics of pollutant concentrations for the three models at urban and rural sites over the 1st January – 30 June 2011, (i) the increment methodology applied over the FR domain (FR_INC), (ii) the CHIMERE high resolution simulation (FR_HRE) and (iii) the CHIMERE low resolution simulation (EU_LRE). The Pearson correlations are rather good for the raw CHIMERE simulations generally in the range 0.7–0.8 for most of pollutants. However, the highest PM concentrations in winter and early spring are underestimated (Fig. 5). For NO_2, differences are clearly identified over the cities and along the major road lines, the root mean square error is systematically improved for this species using a higher resolution (Table 2) mainly due to a reduction of the bias. Ozone concentrations are on average lower using a higher resolution, this is a usual behavior due to the non-linearities in chemistry processes (2^{nd} order kinetic reactions involving ozone).

Table 2
Global error statistics for pollutants concentrations (O_3^{max} is the daily maximum) for the increment methodology (FR_INC), the CHIMERE high resolution simulation (FR_HRE) and the CHIMERE low resolution simulation (EU_LRE) at urban (urb.) and rural (rur.) sites over the 1st January – 30 June 2011 period. Obs. and Pred. are the mean values. Biases, Root Mean Square Error (RMSE) and space and time correlation (Cor.) are based on daily mean values. Bold values are identified to highlight when FR_INC performs as good as or better than the CHIMERE simulation FR_HRE. Refer to Appendix 1 for the definition of error statistics indicators.

Species	Method	Typology	Obs.*	Pred.*	Bias*	RMSE*	Cor.	Numb.
PM10	*FR_INC*	rur	25.73	*15.87*	***-9.85***	***13.78***	*0.77*	*10 233*
	FR_HRE			15.16	-10.56	14.23	0.78	
	EU_LRE			15.64	-10.09	13.69	0.80	
	FR_INC	urb.	27.85	*16.84*	***-11.01***	***15.06***	***0.75***	*29 987*
	FR_HRE			15.93	-11.92	15.69	0.75	
	EU_LRE			15.44	-12.41	15.76	0.78	
PM25	*FR_INC*	rur.	17.69	*12.55*	***-5.13***	***8.99***	***0.83***	*1 565*
	FR_HRE			12.51	-5.18	9.18	0.82	
	EU_LRE			13.86	-3.82	8.19	0.83	
	FR_INC	urb.	20.60	*16.52*	***-4.08***	***10.30***	*0.76*	*10 987*
	FR_HRE			15.64	-4.95	10.54	0.77	
	EU_LRE			15.09	-5.50	9.98	0.82	
NO_2	*FR_INC*	rur.	9.65	*8.96*	***-0.69***	*5.57*	*0.68*	*13 572*
	FR_HRE			7.92	-1.74	5.26	0.71	
	EU_LRE			6.21	-3.45	6.47	0.61	
	FR_INC	urb.	13.04	*11.70*	***-1.33***	*7.47*	*0.63*	*39 520*
	FR_HRE			10.13	-2.91	7.28	0.64	
	EU_LRE			6.41	-6.62	8.86	0.64	
O_3	*FR_INC*	rur.	29.92	*29.67*	***-0.24***	*7.30*	***0.81***	*28 193*
	FR_HRE			30.39	0.47	7.24	0.80	
	EU_LRE			31.56	1.65	7.54	0.79	
	FR_INC	urb.	26.93	*27.95*	***1.02***	***7.59***	*0.77*	*34 977*
	FR_HRE			28.64	1.70	7.61	0.78	
	EU_LRE			31.11	4.18	8.07	0.81	
O_3^{max}	*FR_INC*	rur.	44.27	*40.52*	*-3.75*	*8.82*	***0.86***	*28 618*
	FR_HRE			42.89	-1.38	8.07	0.85	
	EU_LRE			43.60	-0.67	7.59	0.86	
	FR_INC	urb.	41.92	*39.54*	*-2.38*	*8.50*	***0.85***	*35 412*
	FR_HRE			42.25	0.33	7.96	0.85	
	EU_LRE			43.33	1.42	7.94	0.85	

** µg m^{-3} for PM and ppb for gases*

For all pollutants the increment methodology provides very similar results compared to the high resolution simulation, the patterns of mean values over the evaluation period are very close and the average timeseries for all stations in France (Fig. 5) confirm this statement all along the period particularly for PM. For NO_2 concentrations, the increment methodology provides higher NO_2 concentrations over urban areas particularly in winter with coherent lower ozone concentrations due to the titration effect with NO_2. For all pollutants, the bias is improved by the increment methodology with a slight improvement of the Root Mean Square Error while the correlation is sometimes slightly impaired or improved. These results are very satisfactory and could be surprising taking into consideration the simplicity and rough assumptions of this methodology. For PM, the method produces better root mean square errors over the Paris region. The number of data used (*e.g.* up to 39 520 daily values for NO_2) for the evaluation and the diversity of site locations in France is large enough to consider these results statistically representative, a deficiency of the method should have appeared in the error statistics. In the supplementary material, the Quantile-Quantile plots show these good performances particularly for the highest values (Fig. S2 in supplementary material). The main discrepancies of this technique occur for maximum ozone concentrations which become slightly underestimated however this behavior can be explained by the technique that is based on daily values and applied over hourly values with certainly a tendency to smooth the extreme values. However, this smoothing effect is not as large as expected and could be suppressed in the future by some improvements of the methodology. Moreover, for the extreme values, the increment technique provides better performances with values closer to the observations at rural and urban stations compared to the FR_HRE CHIMERE simulation (Fig. S3 in supplementary material). This smoothing effect certainly helps the model to avoid some overshoots due to the extreme sensitivity of this type of air quality model like CHIMERE to the parameterisation of the vertical diffusion coefficient which can be set to an arbitrary minimum value inducing unrealistic stagnant conditions.

In Fig. S4 of the supplementary material additional information on a comparison of the delta of concentration between the increment methodology and the reference high resolution simulation (respectively INC – LRE *versus* HRE – LRE) is provided. The overall statistic parameters are satisfactory with a slope close to 1 and a correlation coefficient between 0.69 for O_3 to 0.84 for NO_2. As anticipated and expected, the intercept is low close to 0. The delta on absolute values represents in the model values from 8 (for O_3) to 12% (for PM) of the total concentration on average. However, for NO_2 concentrations it represents up to 72% in our increment methodology on average compared to 54% in the HRE simulation.

3.2. Possible improvement of the methodology

This first version of the methodology already provides very good results. Such a technique based on first order linear regressions with some selected main physics and chemistry equations is sufficient to provide results as accurate as a usual simulation embedding much more detailed processes. Some improvements will be considered in the next version by investigating the following considerations:

- The use of a 2nd order (or higher) linear regression could be tested for the incremental formula defined in section 2.4 such as:

$$\Delta C_{i,j} = \alpha_{i,j} + \beta_{i,j} \times \widetilde{\Delta C_{i,j}} + \gamma_{i,j} \times \widetilde{\Delta C_{i,j}}^2 \quad (9)$$

with α, β and γ the regression coefficients for grid cell (i,j).

- For ozone, an improvement of the technique depicted in section 2.4.2 could be performed by the use of a multi variable methodology involving at least two predictors (the terms between brackets in Eq. (10)):

$$c^*_{[O_3]i,j} = \alpha_{i,j} + \beta_{i,j} \times \left(\frac{j\tau c_{[NO_2]}}{1 + \tau k_r c_{[NO]}} \right) + \gamma_{i,j} \times \left(\frac{C_{[O_3]B}}{1 + \tau k_r c_{[NO]}} \right) \quad (10)$$

with α, β and γ the regression coefficients for grid cell (i,j).

- The regression techniques could also be defined per quantile of concentrations to improve the results on extreme concentrations.
- More meteorological variables could be implemented in the regression formulas to improve the robustness of the methodology.
- Ozone and nitrogen oxides could be treated by a single methodology to better accounts for their chemical interactions.

The methodology deserves to be tested on finer meshes up to 1 km resolution with an adequate bottom-up emission inventory to confirm these encouraging results and evaluate the linearity of scale dependency. One must keep in mind that the technique must remain simple to make it fast, robust, and the current results are already totally satisfactory for various uses. So far, as it is currently designed, the technique can be applied for short term forecasts, analysis of episodes, long term simulation of past years for mapping. For emission reduction analyses the method is expected to work only for primary PM because primary emissions of PM are taken into account in the methodology. For ozone and more generally secondary pollutants, it could be less straightforward since the change of chemical regime and the VOC (Volatile Organic Compound) chemistry will be not sufficiently considered in the increment technique even through the statistical corrections. However, the sensitivity to emissions and meteorological changes is partially contained in the regression coefficients through the

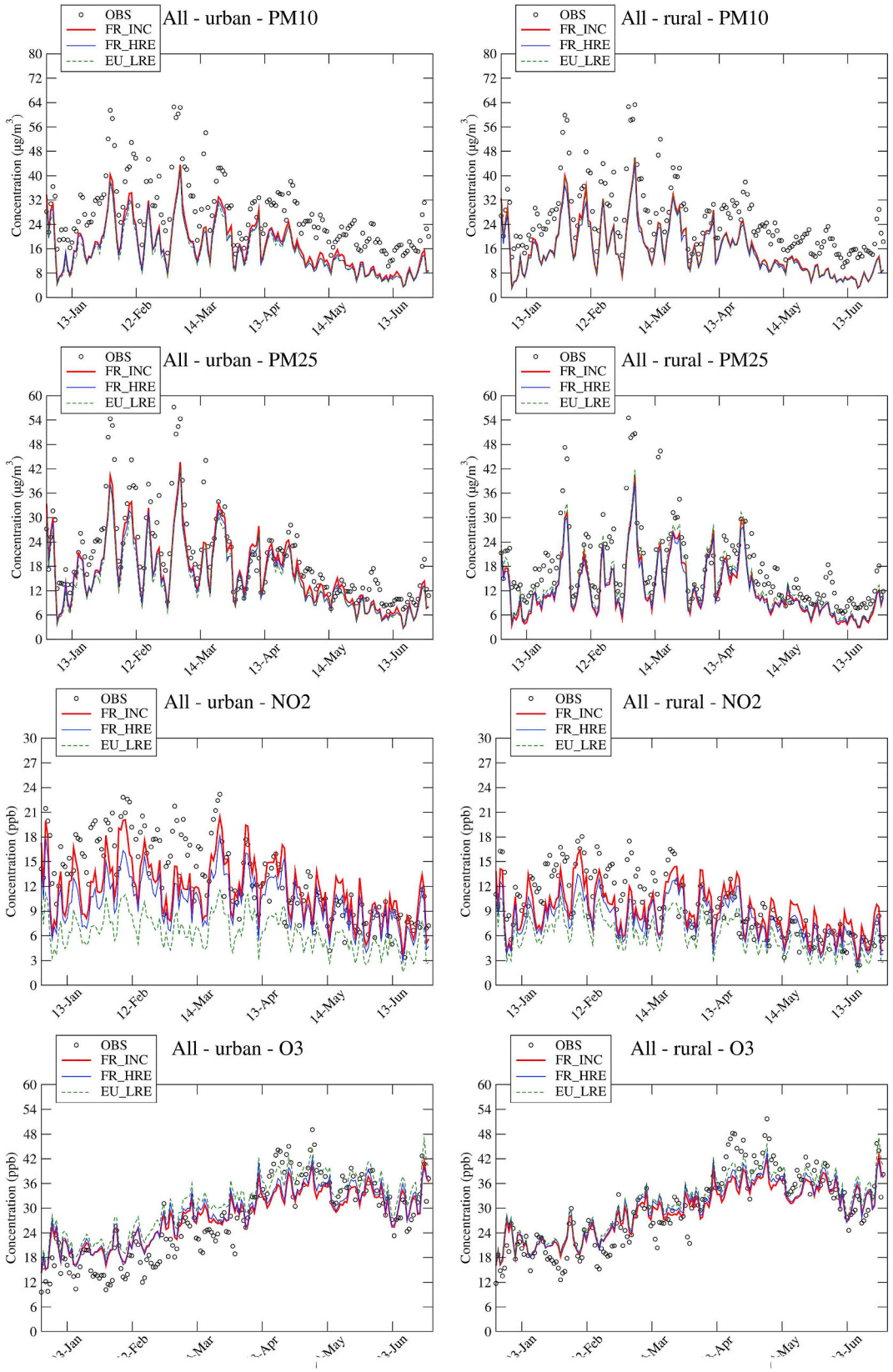

Fig. 5. Timeseries of daily mean PM10, PM2.5, NO_2 and O_3 concentrations for the increment methodology FR_INC, the CHIMERE high resolution simulation FR_HRE and the CHIMERE low resolution simulation EU_LRE mediated at all urban and rural sites over the 1st January – 30 June 2011 period.

diversity of situations encountered over the “training” period.

4. Conclusions

A surrogate model of the CTM CHIMERE has been designed to downscale a coarse horizontal resolution simulation (0.50° × 0.25°) to a finer mesh (0.09375° × 0.046875°). This first version of the methodology is based on a training process over a 6-months period and applied over the subsequent 6 months with an evaluation against the performances of the raw CHIMERE simulation at the highest resolution.

Definitively, our methodology is able to capture the main patterns and evolution of daily concentrations for the main pollutants, and the gain in computing time is very important since the costliest step of the simulation process is by-passed. Performances based on an evaluation against observations are similar to those obtained by the raw model simulations with CHIMERE at high resolution. Performances are even sometimes better certainly due to smoothing effects that suppress some overshoots due to the sensitivity of the model to the parameterizations of the eddy diffusion. Indeed, the vertical diffusion is a very sensitive parameter in CTMs, this coefficient is so sensitive that it is caped in all models and this bounding already results from a kind of ‘learning’ process as it derives from the experience of the model developer during the calibration phase.

In its current state, the methodology can work for short-term air quality forecasts, case studies and air quality concentration mapping. To extend its use to emission reduction assessment, the model could be improved (particularly for Ozone) by (i) implementing additional variables available in the CHIMERE pre-processing, (ii) increasing the order of the linear regression or (ii) the use of multivariable regressions. However, this type of methodology mixing statistics, physics and chemistry is promising and could be run on mono-processor devices and gain a lot of computing time. While the core CHIMERE simulation (step 2) can last several days depending on the number of cores and resolution, only few minutes is sufficient to perform a high resolution simulation with the increment technique, therefore a minimum of 100–1000 less computing times is expected for this step. The training process with NCO procedures lasts about 3 h in our case to fit the regression parameters and this could be optimized with other programming languages. This could open rooms to new fields of research and operational uses in air quality modelling that was so far limited by computing time. These findings will also encourage the CHIMERE development team to parallelize the CHIMERE preprocessing (step 1) to fully take advantage of this technique.

Acknowledgements

This work is partly funded by the French Ministry in charge of Ecology (MTES). The EBAS database has largely been funded by the UN-ECE CLRTAP (EMEP), AMAP and through NILU internal resources. Specific developments have been possible due to projects like EUSAAR (EU-FP5) (EBAS web interface), EBAS-Online (Norwegian Research Council INFRA) (upgrading of database platform) and HTAP (European Commission DG-ENV) (import and export routines to build a secondary repository in support of www.htap.org).

Appendix 1

Error statistics used to evaluate model performance (M and O refer respectively with Model and Observations data, and N is the number of observations).

Bias	$(\bar{M} - \bar{O})$ with $\bar{M} = \frac{1}{N}\sum_{i=1}^{N} M_i$ and $\bar{O} = \frac{1}{N}\sum_{i=1}^{N} O_i$
Root Mean Square Error	$RMSE = \sqrt{\frac{1}{N}\sum_{i=1}^{N}(M_i - O_i)^2}$
Correlation Coefficient	$R = (\sum_{i=1}^{N}(M_i - \bar{M})(O_i - \bar{O}))/\left(\sqrt{\sum_{i=1}^{N}(M_i - \bar{M})^2 \times \sum_{i=1}^{N}(O_i - \bar{O})^2}\right)$

Appendix A. Supplementary data

Supplementary data to this article can be found online at https://doi.org/10.1016/j.envsoft.2019.02.017.

References

Amann, M., Cofala, J., Gzella, A., Heyes, C., Klimont, Z., Schoepp, W., 2007. Estimating Concentrations of Fine Particulate Matter in Urban Background air of European Cities. International Institute for Applied Systems Analysis (IIASA), Laxenburg, Austria IR-07-001. http://pure.iiasa.ac.at/id/eprint/8454/.

Amann, M., Bertok, I., Borken-Kleefeld, J., Cofala, J., Heyes, C., Höglund-Isaksson, L., Klimont, Z., Nguyen, B., Posch, M., Rafaj, P., Sandlera, R., Schöpp, W., Wagnera, F., Winiwarter, W., 2011. Cost-effective control of air quality and greenhouse gases in Europe: modeling and policy applications. Environ. Model. Softw 26, 1489–1501. https://doi.org/10.1016/j.envsoft.2011.07.012.

Amann, M., Purohit, P., Bhanarkar, A.D., Bertok, I., Borken-Kleefeld, J., Cofala, J., Heyes, C., Kiesewetter, G., Klimont, Z., Liu, J., Majumdar, D., Nguyen, B., Rafaj, P., Rao, P.S., Sander, R., Schöpp, W., Srivastava, A., Harsh Vardhan, B., 2017. Managing future air quality in megacities: a case study for Delhi. Atmos. Environ. 161, 99–111. https://doi.org/10.1016/j.atmosenv.2017.04.041.

Anil, D.B., Purohit, P., Rafaj, P., Amann, M., Bertok, I., Cofala, J., Rao, P.S., Vardhan, B.H., Kiesewetter, G., Sander, R., Schöpp, W., Majumdar, D., Srivastava, A., Deshmukh, S., Kawarti, A., Kumar, R., 2018. Managing future air quality in megacities: Co-benefit assessment for Delhi, Atmos. Environ. Times 186, 158–177. ISSN 1352-2310. https://doi.org/10.1016/j.atmosenv.2018.05.026.

Bessagnet, B., Pirovano, G., Mircea, M., Cuvelier, C., Aulinger, A., Calori, G., Ciarelli, G., Manders, A., Stern, R., Tsyro, S., García Vivanco, M., Thunis, P., Pay, M.-T., Colette, A., Couvidat, F., Meleux, F., Rouïl, L., Ung, A., Aksoyoglu, S., Baldasano, J.M., Bieser, J., Briganti, G., Cappelletti, A., D'Isidoro, M., Finardi, S., Kranenburg, R., Silibello, C., Carnevale, C., Aas, W., Dupont, J.-C., Fagerli, H., Gonzalez, L., Menut, L., Prévôt, A.S.H., Roberts, P., White, L., 2016. Presentation of the EURODELTA III intercomparison exercise – evaluation of the chemistry transport models' performance on criteria pollutants and joint analysis with meteorology. Atmos. Chem. Phys. 16, 12667–12701. https://doi.org/10.5194/acp-16-12667-2016.

Bessagnet, B., Menut, L., Colette, A., Couvidat, F., Dan, M., Mailler, S., Létinois, L., Pont, V., Rouïl, L., 2017. An Evaluation of the CHIMERE Chemistry Transport Model to Simulate Dust Outbreaks across the Northern Hemisphere in March 2014. Atmosphere 8, 251. https://doi.org/10.3390/atmos8120251.

Catalano, M., Galatioto, F., 2017. Enhanced transport-related air pollution prediction through a novel metamodel approach. Transport. Res. Transport Environ. 55, 262–276. ISSN 1361-9209. https://doi.org/10.1016/j.trd.2017.07.009.

Colette, A., Bessagnet, B., Meleux, F., Terrenoire, E., Rouïl, L., 2014. Frontiers in air quality modelling. Geosci. Model Dev. (GMD) 7, 203–210. https://doi.org/10.5194/gmd-7-203-2014.

Couvidat, F., Bessagnet, B., Garcia-Vivanco, M., Real, E., Menut, L., Colette, A., 2018. Development of an inorganic and organic aerosol model (CHIMERE 2017β v1.0): seasonal and spatial evaluation over Europe. Geosci. Model Dev. (GMD) 11, 165–194. https://doi.org/10.5194/gmd-11-165-2018.

Düring, I., Bächlin, W., Ketzel, M., Baum, A., Friedrich, U., Wurzler, S., 2011. A new simplified NO/NO2 conversion model under consideration of direct NO2-emissions. Meteorol. Z. 20, 67–73. https://doi.org/10.1127/0941-2948/2011/0491.

Forouzanfar, M.H., Afshin, A., Alexander, L.T., Anderson, H.R., Bhutta, Z.A., Biryukov, S., Brauer, M., Burnett, R., Cercy, K., Charlson, F.J., Cohen, A.J., Dandona, L., Estep, K., Ferrari, A.J., Frostad, J.J., Fullman, N., Gething, P.W., Godwin, W.W., Griswold, M., Hay, S.I., Kinfu, Y., Kyu, H.H., Larson, H.J., Liang, X., Lim, S.S., Liu, P.Y., Lopez, A.D., Lozano, R., Marczak, L., Mensah, G.A., Mokdad, A.H., Moradi-Lakeh, M., Naghavi, M., Neal, B., Reitsma, M.B., Roth, G.A., Salomon, J.A., Sur, P.J., Vos, T., Wagner, J.A., Wang, H., Zhao, Y., Zhou, M., Aasvang, G.M., Abajobir, A.A., Abate, K.H., Abbafati, C., Abbas, K.M., Abd-Allah, F., Abdulle, A.M., Abera, S.F., Abraham, B., Abu-Raddad,

L.J., Abyu, G.Y., Adebiyi, A.O., Adedeji, I.A., Ademi, Z., Adou, A.K., Adsuar, J.C., Agardh, E.E., Agarwal, A., Agrawal, A., Kiadaliri, A.A., Ajala, O.N., Akinyemiju, T.F., Al-Aly, Z., Alam, K., Alam, N.K.M., Aldhahri, S.F., Aldridge, R.W., Alemu, Z.A., Ali, R., Alkerwi, A. 'a, Alla, F., Allebeck, P., Alsharif, U., Altirkawi, K.A., Martin, E.A., Alvis-Guzman, N., Amare, A.T., Amberbir, A., Amegah, A.K., Amini, H., Ammar, W., Amrock, S.M., Andersen, H.H., Anderson, B.O., Antonio, C.A.T., Anwari, P., Ärnlöv, J., Artaman, A., Asayesh, H., Asghar, R.J., Assadi, R., Atique, S., Avokpaho, E.F.G.A., Awasthi, A., Quintanilla, B.P.A., Azzopardi, P., Bacha, U., Badawi, A., Bahit, M.C., Balakrishnan, K., Barac, A., Barber, R.M., Barker-Collo, S.L., Bärnighausen, T., Barquera, S., Barregard, L., Barrero, L.H., Basu, S., Batis, C., Bazargan-Hejazi, S., Beardsley, J., Bedi, N., Beghi, E., Bell, B., Bell, M.L., Bello, A.K., Bennett, D.A., Bensenor, I.M., Berhane, A., Bernabé, E., Betsu, B.D., Beyene, A.S., Bhala, N., Bhansali, A., Bhatt, S., Biadgilign, S., Bikbov, B., Bisanzio, D., Bjertness, E., Blore, J.D., Borschmann, R., Boufous, S., Bourne, R.R.A., Brainin, M., Brazinova, A., Breitborde, N.J.K., Brenner, H., Broday, D.M., Brugha, T.S., Brunekreef, B., Butt, Z.A., Cahill, L.E., Calabria, B., Campos-Nonato, I.R., Cárdenas, R., Carpenter, D.O., Carrero, J.J., Casey, D.C., Castañeda-Orjuela, C.A., Rivas, J.C., Castro, R.E., Catalá-López, F., Chang, J.-C., Chiang, P.P.-C., Chibalabala, M., Chimed-Ochir, O., Chisumpa, V.H., Chitheer, A.A., Choi, J.-Y.J., Christensen, H., Christopher, D.J., Ciobanu, L.G., Coates, M.M., Colquhoun, S.M., Manzano, A.G.C., Cooper, L.T., Cooperrider, K., Cornaby, L., Cortinovis, M., Crump, J.A., Cuevas-Nasu, L., Damasceno, A., Dandona, R., Darby, S.C., Dargan, P.I., das Neves, J., Davis, A.C., Davletov, K., de Castro, E.F., De la Cruz-Góngora, V., De Leo, D., Degenhardt, L., Del Gobbo, L.C., del Pozo-Cruz, B., Dellavalle, R.P., Deribew, A., Jarlais, D.C.D., Dharmaratne, S.D., Dhillon, P.K., Diaz-Torné, C., Dicker, D., Ding, E.L., Dorsey, E.R., Doyle, K.E., Driscoll, T.R., Duan, L., Dubey, M., Duncan, B.B., Elyazar, I., Endries, A.Y., Ermakov, S.P., Erskine, H.E., Eshrati, B., Esteghamati, A., Fahimi, S., Faraon, E.J.A., Farid, T.A., Farinha, C.S. e S., Faro, A., Farvid, M.S., Farzadfar, F., Feigin, V.L., Fereshtehnejad, S.-M., Fernandes, J.G., Fischer, F., Fitchett, J.R.A., Fleming, T., Foigt, N., Foreman, K., Fowkes, F.G.R., Franklin, R.C., Fürst, T., Futran, N.D., Gakidou, E., Garcia-Basteiro, A.L., Gebrehiwot, T.T., Gebremedhin, A.T., Geleijnse, J.M., Gessner, B.D., Giref, A.Z., Giroud, M., Gishu, M.D., Giussani, G., Goenka, S., Gomez-Cabrera, M.C., Gomez-Dantes, H., Gona, P., Goodridge, A., Gopalani, S.V., Gotay, C.C., Goto, A., Gouda, H.N., Gugnani, H.C., Guillemin, F., Guo, Y., Rahul, Gupta, Rajeev, Gupta, Gutiérrez, R.A., Haagsma, J.A., Hafezi-Nejad, N., Haile, D., Hailu, G.B., Halasa, Y.A., Hamadeh, R.R., Hamidi, S., Handal, A.J., Hankey, G.J., Hao, Y., Harb, H.L., Harikrishnan, S., Haro, J.M., Hassanvand, M.S., Hassen, T.A., Havmoeller, R., Heredia-Pi, I.B., Hernández-Llanes, N.F., Heydarpour, P., Hoek, H.W., Hoffman, H.J., Horino, M., Horita, N., Hosgood, H.D., Hoy, D.G., Hsairi, M., Htet, A.S., Hu, G., Huang, J.J., Husseini, A., Hutchings, S.J., Huybrechts, I., Iburg, K.M., Idrisov, B.T., Ileanu, B.V., Inoue, M., Jacobs, T.A., Jacobsen, K.H., Jahanmehr, N., Jakovljevic, M.B., Jansen, H.A.F.M., Jassal, S.K., Javanbakht, M., Jayaraman, S.P., Jayatilleke, A.U., Jee, S.H., Jeemon, P., Jha, V., Jiang, Y., Jibat, T., Jin, Y., Johnson, C.O., Jonas, J.B., Kabir, Z., Kalkonde, Y., Kamal, R., Kan, H., Karch, A., Karema, C.K., Karimkhani, C., Kasaeian, A., Kaul, A., Kawakami, N., Kazi, D.S., Keiyoro, P.N., Kemmer, L., Kemp, A.H., Kengne, A.P., Keren, A., Kesavachandran, C.N., Khader, Y.S., Khan, A.R., Khan, E.A., Khan, G., Khang, Y.-H., Khatibzadeh, S., Khera, S., Khoja, T.A.M., Khubchandani, J., Kieling, C., Kim, C., Kim, D., Kimokoti, R.W., Kissoon, N., Kivipelto, M., Knibbs, L.D., Kokubo, Y., Kopec, J.A., Koul, P.A., Koyanagi, A., Kravchenko, M., Kromhout, H., Krueger, H., Ku, T., Defo, B.K., Kuchenbecker, R.S., Bicer, B.K., Kuipers, E.J., Kumar, G.A., Kwan, G.F., Lal, D.K., Lalloo, R., Lallukka, T., Lan, Q., Larsson, A., Latif, A.A., Lawrynowicz, A.E.B., Leasher, J.L., Leigh, J., Leung, J., Levi, M., Li, X., Li, Y., Liang, J., Liu, S., Lloyd, B.K., Logroscino, G., Lotufo, P.A., Lunevicius, R., MacIntyre, M., Mahdavi, M., Majdan, M., Majeed, A., Malekzadeh, R., Malta, D.C., Manamo, W.A.A., Mapoma, C.C., Marcenes, W., Martin, R.V., Martinez-Raga, J., Masiye, F., Matsushita, K., Matzopoulos, R., Mayosi, B.M., McGrath, J.J., McKee, M., Meaney, P.A., Medina, C., Mehari, A., Mejia-Rodriguez, F., Mekonnen, A.B., Melaku, Y.A., Memish, Z.A., Mendoza, W., Mensink, G.B.M., Meretoja, A., Meretoja, T.J., Mesfin, Y.M., Mhimbira, F.A., Millear, A., Miller, T.R., Mills, E.J., Mirarefin, M., Misganaw, A., Mock, C.N., Mohammadi, A., Mohammed, S., Mola, G.L.D., Monasta, L., Hernandez, J.C.M., Montico, M., Morawska, L., Mori, R., Mozaffarian, D., Mueller, U.O., Mullany, E., Mumford, J.E., Murthy, G.V.S., Nachega, J.B., Naheed, A., Nangia, V., Nassiri, N., Newton, J.N., Ng, M., Nguyen, Q.L., Nisar, M.I., Pete, P.M.N., Norheim, O.F., Norman, R.E., Norrving, B., Nyakarahuka, L., Obermeyer, C.M., Ogbo, F.A., Oh, I.-H., Oladimeji, O., Olivares, P.R., Olsen, H., Olusanya, B.O., Olusanya, J.O., Opio, J.N., Oren, E., Orozco, R., Ortiz, A., Ota, E., PA, M., Pana, A., Park, E.-K., Parry, C.D., Parsaeian, M., Patel, T., Caicedo, A.J.P., Patil, S.T., Patten, S.B., Patton, G.C., Pearce, N., Pereira, D.M., Perico, N., Pesudovs, K., Petzold, M., Phillips, M.R., Piel, F.B., Pillay, J.D., Plass, D., Polinder, S., Pond, C.D., Pope, C.A., Pope, D., Popova, S., Poulton, R.G., Pourmalek, F., Prasad, N.M., Qorbani, M., Rabiee, R.H.S., Radfar, A., Rafay, A., Rahimi-Movaghar, V., Rahman, M., Rahman, M.H.U., Rahman, S.U., Rai, R.K., Rajsic, S., Raju, M., Ram, U., Rana, S.M., Ranganathan, K., Rao, P., García, C.A.R., Refaat, A.H., Rehm, C.D., Rehm, J., Reinig, N., Remuzzi, G., Resnikoff, S., Ribeiro, A.L., Rivera, J.A., Roba, H.S., Rodriguez, A., Rodriguez-Ramirez, S., Rojas-Rueda, D., Roman, Y., Ronfani, L., Roshandel, G., Rothenbacher, D., Roy, A., Saleh, M.M., Sanabria, J.R., Sanchez-Riera, L., Sanchez-Niño, M.D., Sánchez-Pimienta, T.G., Sandar, L., Santomauro, D.F., Santos, I.S., Sarmiento-Suarez, R., Sartorius, B., Satpathy, M., Savic, M., Sawhney, M., Schmidhuber, J., Schmidt, M.I., Schneider, I.J.C., Schöttker, B., Schutte, A.E., Schwebel, D.C., Scott, J.G., Seedat, S., Sepanlou, S.G., Servan-Mori, E.E., Shaddick, G., Shaheen, A., Shahraz, S., Shaikh, M.A., Levy, T.S., Sharma, R., She, J., Sheikhbahaei, S., Shen, J., Sheth, K.N., Shi, P., Shibuya, K., Shigematsu, M., Shin, M.-J., Shiri, R., Shishani, K., Shiue, I., Shrime, M.G., Sigfusdottir, I.D., Silva, D.A.S., Silveira, D.G.A., Silverberg, J.I., Simard, E.P., Sindi, S., Singh, A., Singh, J.A., Singh, P.K., Slepak, E.L., Soljak, M., Soneji, S., Sorensen, R.J.D., Sposato, L.A., Sreeramareddy, C.T., Stathopoulou, V., Steckling, N., Steel, N., Stein, D.J., Stein, M.B., Stöckl, H., Stranges, S., Stroumpoulis, K., Sunguya, B.F., Swaminathan, S., Sykes, B.L., Szoeke, C.E.I., Tabarés-Seisdedos, R., Takahashi, K., Talongwa, R.T., Tandon, N., Tanne, D., Tavakkoli, M., Taye, B.W., Taylor, H.R., Tedla, B.A., Tefera, W.M., Tegegne, T.K., Tekle, D.Y., Terkawi, A.S., Thakur, J.S., Thomas, B.A., Thomas, M.L., Thomson, A.J., Thorne-Lyman, A.L., Thrift, A.G., Thurston, G.D., Tillmann, T., Tobe-Gai, R., Tobollik, M., Topor-Madry, R., Topouzis, F., Towbin, J.A., Tran, B.X., Dimbuene, Z.T., Tsilimparis, N., Tura, A.K., Tuzcu, E.M., Tyrovolas, S., Ukwaja, K.N., Undurraga, E.A., Uneke, C.J., Uthman, O.A., van Donkelaar, A., van Os, J., Varakin, Y.Y., Vasankari, T., Veerman, J.L., Venketasubramanian, N., Violante, F.S., Vollset, S.E., Wagner, G.R., Waller, S.G., Wang, J.L., Wang, L., Wang, Y., Weichenthal, S., Weiderpass, E., Weintraub, R.G., Werdecker, A., Westerman, R., Whiteford, H.A., Wijeratne, T., Wiysonge, C.S., Wolfe, C.D.A., Won, S., Woolf, A.D., Wubshet, M., Xavier, D., Xu, G., Yadav, A.K., Yakob, B., Yalew, A.Z., Yano, Y., Yaseri, M., Ye, P., Yip, P., Yonemoto, N., Yoon, S.-J., Younis, M.Z., Yu, C., Zaidi, Z., Zaki, M.E.S., Zhu, J., Zipkin, B., Zodpey, S., Zuhlke, L.J., Murray, C.J.L., 2016. Global, regional, and national comparative risk assessment of 79 behavioural, environmental and occupational, and metabolic risks or clusters of risks, 1990–2015: a systematic analysis for the Global Burden of Disease Study 2015. Lancet 388, 1659–1724. https://doi.org/10.1016/S0140-6736(16)31679-8.

Fuhrer, O., Chadha, T., Hoefler, T., Kwasniewski, G., Lapillonne, X., Leutwyler, D., Lüthi, D., Osuna, C., Schär, C., Schulthess, T.C., Vogt, H., 2018. Near-global climate simulation at 1 km resolution: establishing a performance baseline on 4888 GPUs with COSMO 5.0. Geosci. Model Dev. 11, 1665–1681. https://doi.org/10.5194/gmd-11-1665-2018.

Kiesewetter, G., Borken-Kleefeld, J., Schöpp, W., Heyes, C., Thunis, P., Bessagnet, B., Terrenoire, E., Gsella, A., Amann, M., 2014. Modelling NO2 concentrations at the street level in the GAINS integrated assessment model: projections under current legislation. Atmos. Chem. Phys. 14, 813–829. https://doi.org/10.5194/acp-14-813-2014.

Kiesewetter, G., Borken-Kleefeld, J., Schöpp, W., Heyes, C., Thunis, P., Bessagnet, B., Terrenoire, E., Fagerli, H., Nyiri, A., Amann, M., 2015. Modelling street level PM10 concentrations across Europe: source apportionment and possible futures. Atmos. Chem. Phys. 15, 1539–1553. https://doi.org/10.5194/acp-15-1539-2015.

Mailler, S., Menut, L., Khvorostyanov, D., Valari, M., Couvidat, F., Siour, G., Turquety, S., Briant, R., Tuccella, P., Bessagnet, B., Colette, A., Létinois, L., Markakis, K., Meleux, F., 2017. CHIMERE-2017: from urban to hemispheric chemistry-transport modeling. Geosci. Model Dev. (GMD) 10, 2397–2423. https://doi.org/10.5194/gmd-10-2397-2017.

Mallet, V., Tilloy, A., Poulet, D., Girard, S., Brocheton, F., 2018. Meta-modeling of ADMS-Urban by dimension reduction and emulation. Atmos. Environ. 184, 37–46. 2018, ISSN 1352-2310. https://doi.org/10.1016/j.atmosenv.2018.04.009.

Menut, L., Bessagnet, B., Khvorostyanov, D., Beekmann, M., Blond, N., Colette, A., Coll, I., Curci, G., Foret, G., Hodzic, A., Mailler, S., Meleux, F., Monge, J.-L., Pison, I., Siour, G., Turquety, S., Valari, M., Vautard, R., Vivanco, M.G., 2013. CHIMERE 2013: a model for regional atmospheric composition modelling. Geosci. Model Dev. (GMD) 6, 981–1028. https://doi.org/10.5194/gmd-6-981-2013.

Ortiz, S.T., Rainer, F., 2013. A modelling approach for estimating background pollutant concentrations in urban areas. Atmos. Poll. Res. 4 (2), 147–156. ISSN 1309-1042. https://doi.org/10.5094/APR.2013.015.

Schaap, M., Cuvelier, C., Hendriks, C., Bessagnet, B., Baldasano, J.M., Colette, A., Thunis, P., Karam, D., Fagerli, H., Graff, A., Kranenburg, R., Nyiri, A., Pay, M.T., Rouïl, L., Schulz, M., Simpson, D., Stern, R., Terrenoire, E., Wind, P., 2015. Performance of European chemistry transport models as function of horizontal resolution. Atmos. Environ. 112, 90–105. https://doi.org/10.1016/j.atmosenv.2015.04.003.

Seinfeld, J., Pandis, S., 1998. Atmospheric Chemistry and Physics - From Air Pollution to Climate Change. Wiley Interscience, New York. https://doi.org/10.1021/ja985605y.

Skamarock, W.C., Park, S.-H., Klemp, J.B., Snyder, C., 2014. Atmospheric Kinetic Energy Spectra from Global High-Resolution Nonhydrostatic Simulations. J. Atmos. Sci. 71, 4369–4381. https://doi.org/10.1175/JAS-D-14-0114.1.

Terrenoire, E., Bessagnet, B., Rouïl, L., Tognet, F., Pirovano, G., Letinois, L., Colette, A., Thunis, P., Amann, M., Menut, L., 2015. High resolution air quality simulation over Europe with the chemistry transport model CHIMERE. Geosci. Model Dev. (GMD) 8, 21–42. https://doi.org/10.5194/gmd-8-21-2015.

Timmermans, R.M.A., Denier van der Gon, H.A.C., Kuenen, J.J.P., Segers, A.J., Honoré, C., Perrussel, O., Builtjes, P.J.H., Schaap, M., 2013. Quantification of the urban air pollution increment and its dependency on the use of down-scaled and bottom-up city emission inventories. Urban Climate 6, 44–62. ISSN 2212-0955. https://doi.org/10.1016/j.uclim.2013.10.004.

Tørseth, K., Aas, W., Breivik, K., Fjæraa, A.M., Fiebig, M., Hjellbrekke, A.G., Lund Myhre, C., Solberg, S., Yttri, K.E., 2012. Introduction to the European Monitoring and Evaluation Programme (EMEP) and observed atmospheric composition change during 1972–2009. Atmos. Chem. Phys. 12, 5447–5481. https://doi.org/10.5194/acp-12-5447-2012.

Trebs, I., Bohn, B., Ammann, C., Rummel, U., Blumthaler, M., Königstedt, R., Meixner, F.X., Fan, S., Andreae, M.O., 2009. Relationship between the NO2 photolysis frequency and the solar global irradiance. Atmos. Meas. Tech. 2, 725–739. https://doi.org/10.5194/amt-2-725-2009.

Troen, I., Mahrt, L., 1986. A simple model of the atmospheric boundary layer: Sensitivity to surface evaporation. Boundary-Layer Meteorol. 37 (1–2), 129–148. https://doi.org/10.1007/BF00122760.

Valari, M., Menut, L., 2008. Does an increase in air quality models resolution bring surface ozone concentrations closer to reality? J. Atmos. Ocean. Technol. 25, 1955–1968. https://doi.org/10.1175/2008JTECHA1123.1.

Van Leer, B., 1979. Towards the ultimate conservative difference scheme. A second order sequel to Godunov's method. J. Comput. Phys. 32, 101–136.

Zender, C.S., 2008. Analysis of self-describing gridded geoscience data with netCDF Operators (NCO). Environ. Model. Softw 23, 1338–1342. https://doi.org/10.1016/j.envsoft.2008.03.004.